


 Cite this: *RSC Adv.*, 2026, 16, 7204

# The application of ICG-based photodynamic therapy combined with nanotechnology in tumor treatment

 Hexin Fu,<sup>a</sup> Lu Zhao<sup>b</sup> and Dong Tang<sup>b,\*c</sup>

Despite remarkable progress in tumor therapy, key challenges—including the immunosuppressive “cold” tumor microenvironment and treatment resistance—remain unresolved and severely impede clinical outcomes. Indocyanine Green (ICG)-based Photodynamic Therapy (PDT), a modality that activates the photosensitizer ICG to generate reactive oxygen species (ROS), has emerged as a pivotal strategy to rewire “cold” tumors into immunologically responsive “hot” tumors, laying the foundation for effective combination therapies. However, PDT itself faces inherent limitations (e.g., poor light penetration, low ROS generation efficiency), and ICG suffers from specific drawbacks (e.g., poor aqueous stability, rapid systemic clearance), collectively restricting their clinical translation. Nanotechnology has become an indispensable tool to address these synergistic challenges, enabling enhanced tumor targeting, prolonged circulation time, and improved ROS generation efficiency of ICG-based PDT. This review summarizes the latest advancements in ICG-based PDT combined with nanotechnology for cancer treatment and discusses its potential and challenges in synergizing with chemotherapy and immunotherapy to amplify antitumor efficacy.

 Received 6th November 2025  
 Accepted 4th January 2026

DOI: 10.1039/d5ra08557h

[rsc.li/rsc-advances](https://rsc.li/rsc-advances)

## 1. Introduction

Despite significant advances in medicine and technology, cancer remains one of the most challenging global public health issues. According to the most recent global cancer statistics (GLOBOCAN 2022, published in 2024) released by the International Agency for Research on Cancer (IARC), there were approximately 20 million new cancer cases (including non-melanoma skin cancer) and 9.7 million cancer-related deaths worldwide annually, accounting for 22.8% and 30.3% of global non-communicable disease (NCD) deaths, respectively. Approximately 1 in 5 men or women will develop cancer in their lifetime, while 1 in 9 men and 1 in 12 women will die from the disease. Lung cancer (12.4% of new cases, 18.7% of deaths) is the most common and lethal cancer globally, followed closely by female breast cancer, colorectal cancer, prostate cancer, and gastric cancer in terms of incidence. Lung cancer has ranked

first in global cancer mortality for 10 consecutive years, with colorectal cancer, liver cancer, female breast cancer, and gastric cancer also among the top five leading causes of cancer death. Based on projections of population growth and aging, the number of new global cancer cases is expected to rise to 35 million by 2050, a 77% increase from 2022, with lung cancer, breast cancer, and colorectal cancer remaining the major disease burdens.<sup>1</sup> While cancer treatments are constantly evolving, with targeted therapy and immunotherapy gaining considerable attention in recent years, these approaches still have their limitations.<sup>2</sup> The tumor microenvironment is typically characterized by hypoxia, acidity, and immune suppression, commonly referred to as “cold” tumors, which severely limit treatment efficacy and patient survival rates.<sup>3</sup>

PDT has emerged in recent years as a relatively non-invasive treatment method, offering a novel localized targeted therapy approach. Initially, PDT was primarily used for the treatment of skin diseases.<sup>4</sup> In 1942, Auler and Figge first discovered the photodynamic cytotoxic effect of hematoporphyrin on tumor tissue, marking the beginning of PDT's application in cancer treatment.<sup>5</sup> In simple terms, PDT involves irradiating a photosensitizer that accumulates in diseased tissue with light of a specific wavelength, which generates singlet oxygen or other free radicals. These reactive species interact with surrounding tissue, inducing a series of necrosis, apoptosis, and autophagy processes in the diseased tissue to achieve therapeutic removal.<sup>6</sup> Beyond this direct cell killing, the therapeutic damage itself initiates a potent immunostimulatory effect. This process

<sup>a</sup>Northern Jiangsu People's Hospital Affiliated to Yangzhou University, Yangzhou, 225000, China. E-mail: 431245408@qq.com

<sup>b</sup>The Yangzhou Clinical Medical College of Xuzhou Medical University, Yangzhou, 225001, China

<sup>c</sup>Department of General Surgery, Institute of General Surgery, Northern Jiangsu People's Hospital Affiliated to Yangzhou University, Northern Jiangsu People's Hospital, The Yangzhou Clinical Medical College of Xuzhou Medical University, The Yangzhou School of Clinical Medicine of Dalian Medical University, The Yangzhou School of Clinical Medicine of Nanjing Medical University, Northern Jiangsu People's Hospital, Clinical Teaching Hospital of Medical School, Nanjing University, Yangzhou, 225000, China. E-mail: 83392785@qq.com; Tel: +86-18952783556



converts the immunosuppressive 'cold' tumor into an immunologically 'hot' one by exposing tumor antigens and triggering an inflammatory response. Compared to traditional treatment methods, PDT exhibits unique advantages in the treatment of various cancers, particularly demonstrating remarkable efficacy against superficial, early-stage tumors and those located in vital functional organs.<sup>7</sup> Its minimally invasive nature, precise targeting ability, and organ function-preserving characteristic are advantages unparalleled by traditional therapies. For instance, PDT achieves a complete response rate (CRR) of 79.9–96.7% in the treatment of early-stage oral, pharyngeal, and laryngeal cancers while preserving organ function, as well as speech and swallowing functions.<sup>8</sup> The 2020 Expert Consensus on the Clinical Application of Photodynamic Therapy for Esophageal Cancer confirms that PDT can achieve a curative effect for early-stage esophageal cancer, with a 5 year survival rate exceeding 85%. Among lung cancer—the most prevalent and lethal cancer globally—bronchoscopic-guided PDT for early-stage central lung cancer can completely eradicate intraluminal tumors and preserve lung function, making it particularly suitable for patients who are not candidates for surgical resection.<sup>9</sup> ICG is one of the most commonly used second-generation near-infrared (NIR) photosensitizers in PDT and is currently the only NIR fluorescent dye approved by the U.S. Food and Drug Administration (FDA) for clinical use. It has been widely applied in diagnosis.<sup>10</sup> While ICG is clinically approved worldwide as a near-infrared fluorescent diagnostic agent for various applications (such as hepatic function assessment, ophthalmic angiography, and sentinel lymph node mapping), its specific use in PDT for cancer treatment is currently considered an investigational therapy and has not yet received broad clinical approval. ICG possesses superior optical properties for biomedical applications. Its peak absorption and emission lie within the NIR range (approximately 800 nm). This is critically important because biological tissues exhibit a characteristic "optical window" in the NIR spectrum (roughly 650–1350 nm), where the combined absorption of hemoglobin, melanin, and water is at its minimum. Consequently, NIR light can penetrate tissues more deeply than visible light, facilitating the diagnosis and treatment of deeper-seated lesions (Table 1).

However, the clinical translation of ICG agents necessitates a thorough consideration of their stability, clearance, and toxicity profiles. ICG, while clinically approved, suffers from inherent limitations in aqueous stability, including concentration-dependent aggregation, thermal degradation, and rapid photobleaching upon light irradiation. These factors can significantly compromise its singlet oxygen quantum yield and therapeutic efficacy. Many formulations strategy, which involves encapsulating ICG within nanoparticles, aims to mitigate these issues. The nanoparticles shield the encapsulated ICG from the aqueous environment, potentially reducing molecular aggregation and retarding its photodegradation, thereby enhancing its shelf-life and photostability during treatment.<sup>11</sup> Regarding the *in vivo* fate, free ICG is known to bind rapidly to plasma proteins, such as albumin, and is primarily cleared by the hepatobiliary system with a short plasma half-life. This rapid clearance can limit its tumor

accumulation. The nano-formulation may alter the pharmacokinetics and biodistribution of ICG. The enhanced permeability and retention (EPR) effect could facilitate the preferential accumulation of our ICG-loaded nanoparticles in the tumor tissue, potentially prolonging its circulation time and enhancing the therapeutic window for PDT.<sup>12</sup> Concerning toxicity, ICG itself has an excellent safety record in clinical diagnostics at recommended doses. Previous studies have indicated that ICG exhibits low dark toxicity *in vitro* and *in vivo*. Nanoparticles are designed to further minimize any systemic toxicity by targeting the release of ICG and cytotoxic ROS predominantly at the tumor site. Future studies will include comprehensive toxicological assessments to fully validate the safety of nano-formulation.<sup>13</sup>

Although PDT has made significant advancements, its inherent limitations, such as poor light penetration, low ROS generation efficiency, and photosensitizer characteristics, continue to restrict its therapeutic effectiveness. Light source is also a problem that needs to be urgently solved. The efficacy of PDT is intrinsically linked to the effective delivery of light to the target tissue, which remains a primary consideration in its clinical application. The choice of light delivery strategy is dictated by the tumor's anatomical location. For superficial lesions, such as skin cancer, direct surface illumination is straightforward. For internal cavities (*e.g.*, esophageal, bladder, or bronchial cancers), light is delivered *via* flexible endoscopes equipped with optical fibers. For deeper, solid tumors, interstitial PDT is employed, wherein optical fibers tipped with cylindrical diffusers are inserted directly into the tumor mass under image guidance. A key limitation is the rapid attenuation of light in biological tissue, restricting the effective treatment depth to a few centimeters and making the eradication of large or deeply seated tumors challenging. Furthermore, complex anatomical paths can make uniform light distribution difficult. Recent progress is actively addressing these hurdles. Advances include the development of more flexible and miniaturized light sources for improved access, the integration of real-time imaging (*e.g.*, MRI, fluorescence) to monitor and guide light application, and the exploration of novel paradigms such as wireless, implantable micro-light-emitting diodes (micro-LEDs).

Fortunately, numerous studies have explored the use of nanotechnology to address these limitations. Nanomedicine was initially developed to enhance tumor uptake of chemotherapeutic drugs and reduce off-target toxicity.<sup>14</sup> Today, it is primarily used to deliver chemotherapeutic agents, enhance the efficacy of immunotherapy, gene therapy, and photothermal therapy.<sup>15</sup> The small size and large surface area-to-volume ratio of nanoparticles allow them to efficiently absorb, bind, and deliver small molecules,<sup>16</sup> enabling precise and efficient delivery of therapeutic agents to target tissues, cells, or organs while minimizing the risk of side effects.<sup>17</sup> Combining PDT with nanotechnology can significantly enhance PDT efficacy. Based on the latest research progress and our study background, the loading of ICG with bioactive materials/nanomaterials mainly relies on four core mechanisms: electrostatic interaction, hydrophobic encapsulation, covalent conjugation, and



Table 1 Comparative table of core properties of commonly used photosensitizers

Photosensitizer	Chemical class	Maximum absorption wavelength	Molecular weight	Water solubility	<i>In vivo</i> half-life	Photostability	Tissue penetration depth	Clinical advantages	Approval status
Indocyanine green (ICG)	Tricarbocyanine dye	780–805 nm	775 Da	Moderate	150–180 seconds	Low	Deepest (7–10 mm)	First approved medical fluorescent dye; safe (negligible toxicity, liver excretion, 3–5 min half-life); expanded to minimally invasive navigation, widely used intraoperative tracer	FDA-approved for imaging
Porfimer sodium (photofrin)	Hematoporphyrin derivative	630 nm	~1500 Da (mixture)	Low	48–72 hours	High	Shallow (2–3 mm)	First commercialized photosensitizer (hematoporphyrin derivative); palliative efficacy in esophageal/bronchogenic carcinoma; FDA orphan drug (1989) for accelerated approval	FDA-approved for PDT
Temoporfin (mTHPC/Foscan)	Chlorin	652–655 nm	660 Da	Very low	5–7 days	High	Moderate (3–5 mm)	Second-generation photosensitizer; longer wavelength (652 nm)/deeper penetration (5–7 mm) vs. Photofrin; EU phase III efficacy; low dose (0.15 mg kg <sup>-1</sup> ); defined photoactivation	EU-approved for PDT
5-Aminolevulinic acid (ALA)	Porphyrin precursor	635 nm	161 Da	High	3–6 hours	Moderate	Shallow (1–2 mm)	Endogenous heme precursor; converts to PpIX (malignant-selective accumulation); oral formulation (FDA orphan/Fast track); improves glioma resection	FDA-approved for PDT

mesoporous adsorption (Fig. 1). For example, aminated nanodiamonds (modified with ethylenediamine or propylenediamine) carry positive charges on their surface, which form electrostatic attraction with the negatively charged ICG molecules, enabling efficient loading. In addition, liposomes prepared by microfluidic technology encapsulate ICG in their hydrophobic interior, which improves ICG's stability and extends its blood circulation half-life from 3–4 minutes to 4.2 hours. Regardless of the binding method, both components enhance PDT efficacy through multiple mechanisms. Firstly, systemic delivery of these nano-formulations facilitates passive tumor targeting *via* the EPR effect, a phenomenon pioneered by Maeda and colleagues, whereby nanomedicines preferentially extravasate and accumulate in tumor tissue due to its leaky vasculature and impaired lymphatic drainage.<sup>18</sup> Beyond

improved targeting, the nanocarrier shields the encapsulated ICG from the aqueous environment, mitigating its molecular aggregation and enhancing its photostability, thereby maximizing singlet oxygen generation. Furthermore, the nano-platform promotes increased cellular uptake and prolonged retention of the photosensitizer within the tumor, and can be engineered for controlled release or co-delivery of adjuvants (*e.g.*, immune checkpoint inhibitors) to enable potent combination therapies.<sup>19</sup>

Existing literature on ICG-mediated PDT has systematically elaborated on the inherent limitations of photosensitizers and PDT, as well as the advancements in nanotechnology. However, these studies fail to achieve in-depth integration of ICG-PDT with nanotechnology, and discussions on its synergistic effects with chemotherapy/immunotherapy remain relatively



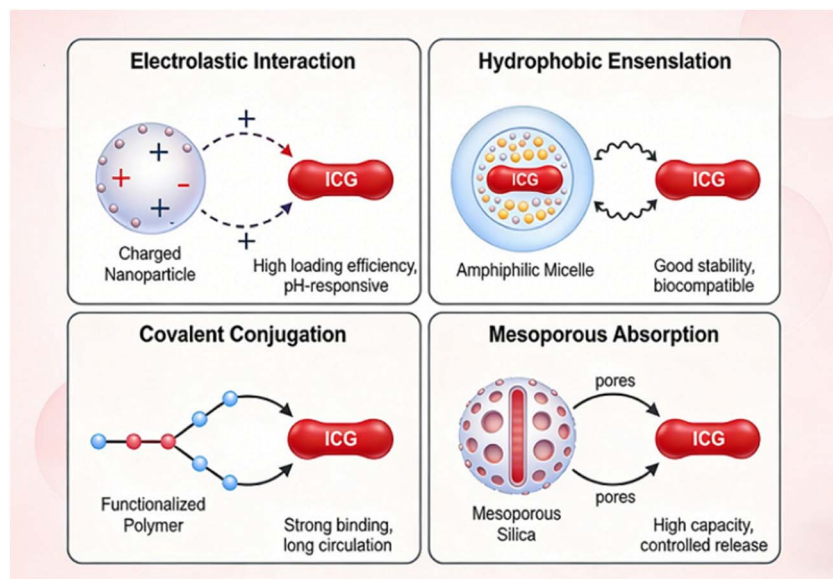


Fig. 1 Schematic diagram of the loading mechanism between ICG and nanomaterials.

scattered. In contrast, this review focuses on tumor therapy, systematically correlating the limitations of ICG, the “cold tumor to hot tumor” conversion function of PDT, and the targeted optimization solutions of nanotechnology. It clarifies the integrated synergistic mechanism of “ICG-PDT + nanotechnology + chemotherapy/immunotherapy” and highlights clinical value by addressing key translational bottlenecks, thereby filling the gaps in existing research.

To ensure a comprehensive and systematic overview of the field, a rigorous literature search and selection process was employed. The primary electronic databases consulted for this review included PubMed, Web of Science Core Collection, and Scopus. The search strategy utilized a combination of key terms and Boolean operators, such as (“Indocyanine Green” OR ICG) AND (“Photodynamic Therapy” OR PDT) AND (nanoparticle OR nano OR nanomedicine) and (cancer OR tumor OR oncology). The search was focused on articles published between January 2019 and May 2024 to capture the most relevant advancements.

## 2. Mechanisms of ICG-based PDT

The three key components of PDT are the light source, photosensitizer, and oxygen. After administration, the photosensitizer ICG is distributed throughout the body *via* the bloodstream and accumulates significantly in tumor tissues. Upon absorbing energy from a specific light source, ICG becomes activated and transfers energy to surrounding oxygen molecules, generating cytotoxic singlet oxygen that damages tumor cells. This is the primary mechanism of action for PDT alone.<sup>20</sup> However, a more crucial mechanism is the immune enhancement induced by PDT, which promotes the transformation of the tumor microenvironment from a “cold” to a “hot” state, increasing treatment efficacy.

### 2.1 Direct cytotoxic effects of PDT

The light source is the trigger point for PDT, and the wavelength of light determines whether it can activate the photosensitizer to produce ROS. When light is applied to tissues, it undergoes reflection, transmission, and absorption, which weakens the light and prevents it from reaching deeper tissues.<sup>21</sup> This is where the NIR photosensitizer ICG surpasses other photosensitizers. The NIR wavelength has stronger tissue penetration, allowing more photosensitizers to be activated and generating more ROS, thus achieving better effects on tumors located in deeper tissues. Once the photosensitizer absorbs photons and transitions to an excited state, it can either return to its ground state *via* fluorescence emission or become further excited to a triplet state. These two processes lead to two distinct reaction types, known as Type I and Type II reactions.<sup>22</sup> In Type I reactions, electrons or protons are transferred to surrounding molecules, forming a large number of free radicals. These free radicals can react further with oxygen to generate ROS, including hydroxyl radicals and hydrogen peroxide. In contrast, Type II reactions involve the direct transfer of energy from the triplet-state photosensitizer to surrounding oxygen molecules, converting them into excited singlet oxygen.<sup>20</sup> Although both reactions can occur simultaneously to produce ROS that cause irreversible damage to tumor tissue, studies have shown that singlet oxygen is the primary mediator of PDT-induced biological damage. Thus, Type II reactions are considered the dominant process. Moreover, the diffusion distance of singlet oxygen in Type II reactions is relatively short, meaning that biological effects can only occur in the regions where the photosensitizer is activated.<sup>23</sup> This characteristic contributes to the strong specificity of PDT.

Currently, the detection methods for ROS in PDT have formed a multi-dimensional technical system. Among these, fluorescent probe-based detection is the most widely used:



DCFH-DA can quantify intracellular total ROS through hydrolysis and oxidation reactions; SOSG specifically recognizes singlet oxygen ( $^1\text{O}_2$ ); and probes such as DHE and MitoSOX Red enable accurate detection of specific ROS subtypes like superoxide anion. Owing to their high sensitivity and convenience, these probes have become the preferred choice for ROS evaluation at the cellular level. As the “gold standard” for free radical detection, Electron Spin Resonance (ESR/EPR) spectroscopy utilizes spin traps (e.g., DMPO, TEMP) to form stable adducts with short-lived free radicals, allowing direct differentiation of ROS types such as  $\cdot\text{OH}$  and  $^1\text{O}_2$ , and providing direct evidence for identifying Type I/Type II reaction pathways in PDT. In addition, chemiluminescence achieves real-time ROS monitoring and high-throughput screening by leveraging the luminescent signals of reagents like luminol; high-performance liquid chromatography (HPLC) enables accurate quantification of ROS in complex biological samples through detecting ROS-induced oxidative products; and Raman spectroscopy (especially surface-enhanced Raman spectroscopy, SERS) and multifunctional nanoprobe technologies have further broken through the limitations of traditional detection methods, realizing simultaneous identification of multiple ROS subtypes, *in vivo* real-time visualization, and non-invasive monitoring. The rational combination of these methods (e.g., complementarity between fluorescent probe-based detection and ESR/EPR spectroscopy) can effectively improve the accuracy and comprehensiveness of ROS detection, providing strong technical support for mechanism research, photosensitizer screening, and clinical efficacy evaluation in PDT (Table 2).

## 2.2 Tumor cell death mediated by cellular signaling pathways

Tumor cells can undergo two types of death: necrosis and apoptosis. The outcome is determined by factors such as the nature of the photosensitizer, the wavelength and power of radiation, and tissue oxygen concentration. Research evidence suggests that low-dose PDT primarily induces apoptosis, while high-dose PDT tends to cause necrosis. Necrosis induced by PDT is dependent on pathways such as the c-Jun N-terminal

kinase (JNK) cascade.<sup>24</sup> ROS generated during PDT can directly damage the integrity of organelles and cell membranes, and photosensitizers localized to organelles such as the endoplasmic reticulum and Golgi apparatus can generate singlet oxygen, leading to cell necrosis.<sup>25</sup> PDT mainly induces tumor cell apoptosis through endogenous signaling pathways.<sup>19</sup> Most photosensitizers in PDT are localized in the mitochondria, where they disrupt mitochondrial function, leading to the release of cytochrome C. Cytochrome C then forms a complex with apoptotic protease activating factor-1 (Apaf-1) and further binds with caspase-9 to form the apoptosome, which induces tumor cell apoptosis.<sup>26</sup> Additionally, phospholipase A2 and phospholipase C are activated by PDT and participate in signal transduction, leading to a significant release of  $\text{Ca}^{2+}$ , which further facilitates apoptosis.<sup>20</sup> Studies have also shown that autophagy regulated by the phosphatidylinositol-3-kinase (PI3K) signaling pathway plays a crucial role in PDT-induced cell death.<sup>27</sup>

## 2.3 PDT promotes the transformation of “cold” tumors into “hot” tumors

PDT not only controls tumor growth by directly killing tumor cells but also modulates the tumor microenvironment, promoting the recruitment and activation of immune cells. This process facilitates the transformation of immune “cold” tumors into “hot” tumors (Fig. 2).

**2.3.1 Induction of immunogenic cell death, release of tumor-associated antigens, and activation of antigen-presenting cells.** PDT induces immunogenic cell death (ICD) in tumor cells by generating ROS, promoting the release of tumor-associated antigens (TAAs), which serve as the trigger for subsequent immune responses.<sup>28</sup> Following tumor cell death, DAMPs, such as ATP, high mobility group box 1 (HMGB1), and calreticulin, are released. These DAMPs attract and activate dendritic cells (DCs) and facilitate the uptake of tumor antigens.<sup>29</sup> Mature DCs then deliver the antigens to lymph nodes, where they activate  $\text{CD8}^+$  T cells, initiating an adaptive anti-tumor immune response. Activated T cells can effectively recognize and kill tumor cells, which is essential for sustaining

Table 2 Comprehensive comparison of ROS detection methods in photodynamic therapy

Detection method	Fluorescence target	Sensitivity	Specificity	Real-time monitoring	Operation complexity	Application scenarios
DCFH-DA fluorescence assay	Total ROS	High ( $\sim 10^{-7}$ M)	Moderate (pan-ROS)	Yes	Low	Intracellular total ROS quantification; high-throughput screening
SOSG fluorescence assay	Singlet oxygen ( $^1\text{O}_2$ )	High ( $\sim 10^{-8}$ M)	Extremely high ( $^1\text{O}_2$ -specific)	Yes	Low	$^1\text{O}_2$ detection in PDT; photosensitizer evaluation
ESR/EPR spin trapping	Specific free radicals	Extremely high ( $\sim 10^{-9}$ M)	Extremely high (radical-type distinguishable)	No (sample required)	High	Free radical type identification; type I/type II PDT differentiation
Chemiluminescence assay	Multiple ROS	Extremely high ( $\sim 10^{-10}$ M)	Moderate	Yes	Moderate	Real-time monitoring; high-throughput screening
HPLC-MS	Specific ROS derivatives	High	Extremely high	No	High	Accurate ROS quantification in complex biological samples



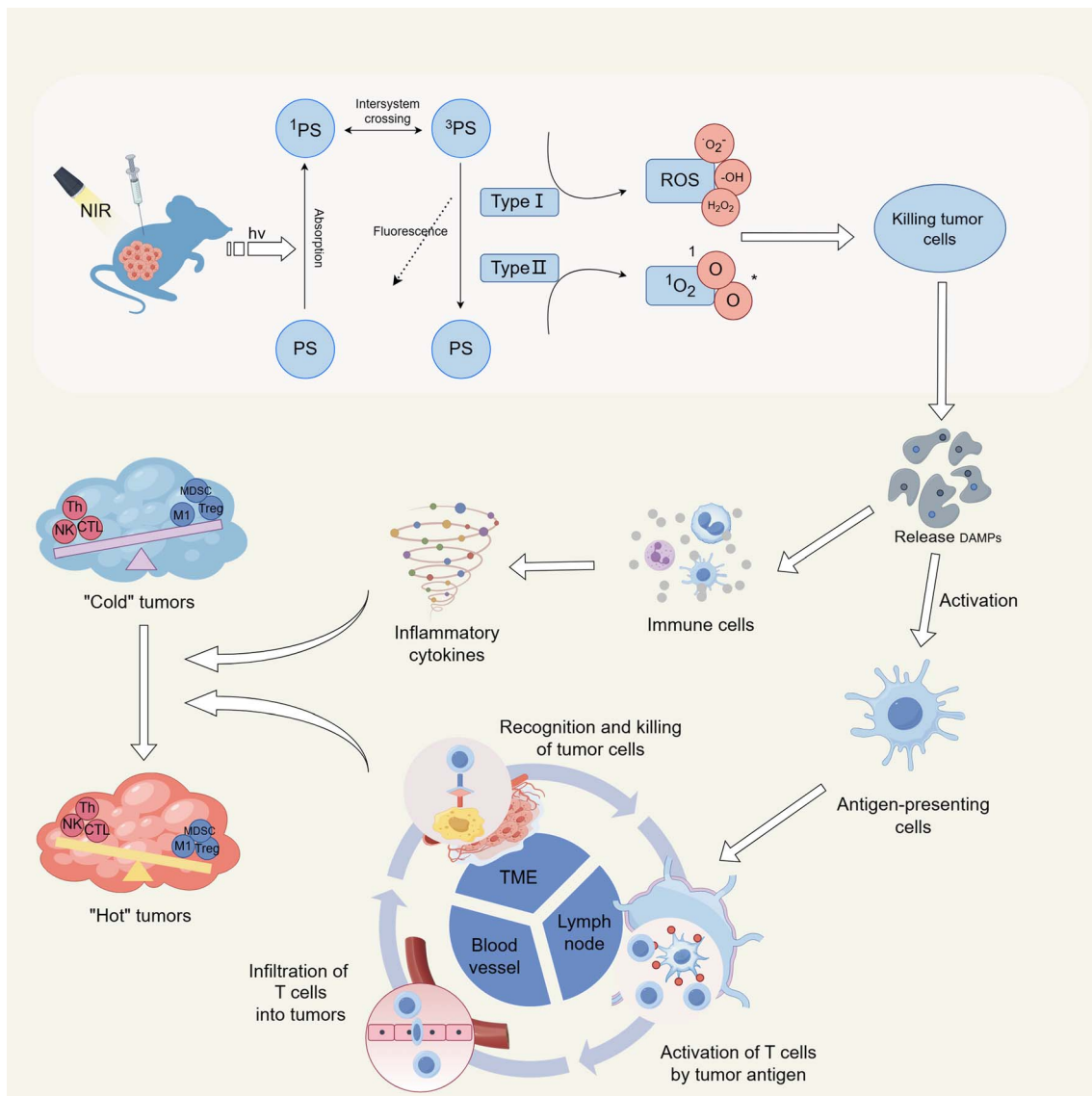


Fig. 2 The main mechanism of PDT. The photosensitizer absorbs energy and jumps from the ground state to a singly excited state and then to a triply excited state. In the type I reaction, photosensitizer excitation generates radical ions or further reaction of radicals with molecular oxygen to produce various ROS. In the type II reaction, the triply excited state of the photosensitizer transfers energy directly to molecular oxygen to form the singly excited state of oxygen. TAAs and DAMPs released after tumor cell death not only activate antigen-presenting cells, which in turn activate T cells and initiate adaptive immunity, but also trigger an inflammatory response that recruits a large number of immune cells and promotes their release of inflammatory factors.

long-term antitumor immunity.<sup>30</sup> This T-cell-mediated immune response significantly enhances the immune activity of the tumor, converting immune “cold” tumors into “hot” tumors.

**2.3.2 Induction of local inflammatory response and promotion of immune cell infiltration.** Following PDT treatment, the ROS and DAMPs generated in the local tumor microenvironment not only induce tumor cell death but also trigger an inflammatory response that attracts a large number of immune cells to infiltrate the tumor region.<sup>31</sup> Innate immune cells, such as macrophages, dendritic cells, and neutrophils, are recruited to the tumor site, where they help clear PDT-damaged tumor cells and release pro-inflammatory cytokines, including tumor necrosis factor- $\alpha$  (TNF- $\alpha$ ), interleukin-6 (IL-6), and

interleukin-1 $\beta$  (IL-1 $\beta$ ).<sup>32</sup> The release of these inflammatory cytokines further enhances the immune activity within the tumor microenvironment, facilitating the transformation of immune “cold” tumors into “hot” tumors.

**2.3.3 Disruption of the tumor vascular barrier and enhancement of immune cell infiltration.** The tumor microenvironment typically contains abnormal vascular structures that often impede immune cell infiltration into the tumor.<sup>33</sup> Studies have shown that PDT can disrupt the tumor's vascular structure, increasing vascular permeability and improving blood flow. This significantly enhances the infiltration of immune cells, particularly T cells, into the tumor, thereby boosting immune activity within the local microenvironment.<sup>34</sup>



### 3. Advances in research on ICG-based PDT combined with nanotechnology

The efficacy of PDT is severely limited by factors such as tissue depth and oxygen levels within tissues. With the development of nanomedicine, numerous nanoplatforms have been established to enhance the antitumor effects of PDT. These platforms primarily focus on overcoming challenges such as the limited penetration of light in tissues, the hypoxic tumor microenvironment, and improving the tumoricidal effects of ROS,<sup>35</sup> and considerable progress has been made in this area (Fig. 3). The main goal of nanomedicine here is to develop a safe and effective drug delivery system that selectively targets tumor cells without harming normal cells.<sup>36</sup> Due to their excellent biological properties, good circulation capabilities, high drug encapsulation efficiency, and ease of functionalization, nanomaterials have significantly advanced research in cancer treatment.<sup>37</sup>

#### 3.1 Functional recombination of ICG with organic nanomaterials

Organic nanomaterials have been widely applied in overcoming the inherent limitations of PDT due to their low energy consumption, renewability, low density, and biodegradability. Common nanocarriers include liposomes, polymer nanoparticles, calcium carbonate nanoparticles, silica nanoparticles, and carbon-based nanomaterials.<sup>38</sup> These carriers not only improve the stability of the photosensitizer ICG but also enhance the overall antitumor efficacy of PDT (Table 3).

Among carbon-based nanomaterials, carbon quantum dots (CQDs) have garnered significant attention due to their low toxicity, high water solubility, high photostability, and high quantum yield.<sup>39</sup> Studies have shown that the combination of CQDs with ICG can enhance ICG's photosensitizing effects and allow for controlled release in the acidic tumor microenvironment.<sup>40</sup> Under laser irradiation, ICG is gradually released from CQD nanoparticles, producing ROS and significantly increasing tumor cell damage. Additionally, CQDs can inhibit ICG leakage under physiological pH, further improving the therapeutic effect.<sup>41</sup>

In nanomedicine research, intravenous administration often results in reduced drug accumulation at the target site due to capture by the reticuloendothelial system (RES).<sup>42</sup> To address this issue, researchers have employed biological proteins or peptides to modify nanoparticles, enhancing their biocompatibility and tumor-targeting properties. For example, ICG has been loaded into heavy-chain ferritin (HFn) nanocages,<sup>43</sup> which target tumor cells by binding to the highly expressed transferrin receptor (TfR1) on cancer cells,<sup>44</sup> improving drug delivery efficiency to tumors. Moreover, ICG treatment and irradiation lead to gene mutations and significantly increase endogenous H-Fn levels in cells, further promoting the uptake of exogenous HFn, thereby enhancing the antitumor effect.<sup>43</sup> Similarly, glycolipid-like micelles modified with cyclic Arg-Gly-Asp peptide (c(RGDfk)) have demonstrated excellent targeting capability and antitumor potential.<sup>45</sup> The c(RGDfk) cyclic peptide specifically binds to integrin  $\alpha_v\beta_3$ , a highly expressed adhesion molecule on the surface of endothelial cells in newly formed blood vessels, inhibiting endothelial cell proliferation and blocking angiogenesis.<sup>46</sup> Under near-infrared light irradiation, this system

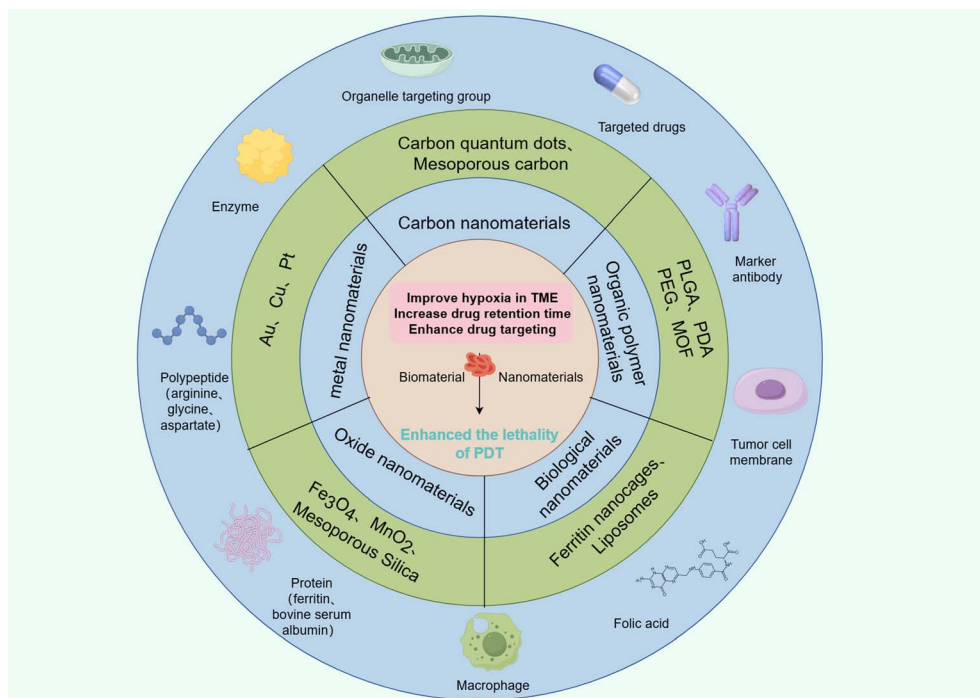


Fig. 3 Commonly used nanomaterials and modifiers. The inner circle of the figure shows commonly used nanomaterials and their classification, and the outer circle the modification methods commonly used in research to enhance the efficacy of nanomedicines.



Table 3 Organic nanodrugs loaded with ICG

Researchers	Strategy	Nanomaterials	Tumor cell-targeting ligands	Loaded drugs	Photosensitizer	Laser parameters	Experimental results	Reference
Hadiseh Mehravanfar	Functional recombination of ICG and organic materials	CQD	—	—	ICG	808 nm, 2.0 W cm <sup>-2</sup> , 3 min	Significantly kills B16F10 melanoma cells (survival 28%), enhances tumor accumulation in C57BL/6 mice, inhibits tumor growth with good biocompatibility	40
Leopoldo Sitia		Heavy ferritin nanocages	TfR1	—	ICG	808 nm, 1.0 W cm <sup>-2</sup> , 3 min	TfR1-mediated targeting of breast cancer cells, better killing on BT-474 (high TfR1), enables tumor fluorescence imaging, good biocompatibility	43
Yupeng Liu		Micelle	c(RGDfk)	—	ICG	808 nm, 2.0 W cm <sup>-2</sup> , 3 min	Dual-targets U87 MG cells and HUVECs, 80% tumor inhibition in nude mice, reduces tumor vessels, induces apoptosis, no organ toxicity	45
Zhiting Sun		PLGA	L-Arg	—	ICG	—	Kills 4T1 cells, induces apoptosis/necrosis, degrades tumor collagen I, sustained drug release, inhibits tumor growth with excellent biocompatibility	47
Jing Liu		TAT	HAS, TAT	—	ICG	808 nm, 2.0 W cm <sup>-2</sup> , 5 min	Enhances nuclear targeting in 4T1 cells, generates <sup>1</sup> O <sub>2</sub> /heat, induces apoptosis/DNA damage, ablates tumors, no blood/organ abnormalities	50
Xiudan Wang		Mesoporous carbon	FA, macrophage	—	ICG	808 nm, 2.0 W cm <sup>-2</sup> , 3 min	Macrophage-mediated tumor delivery, M1 polarization, 2x higher tumor accumulation, synergistic PDT/PTT/immunotherapy, good biocompatibility	52
Yuanwei Zhang	Combination therapy with loaded chemotherapy drugs	Mesoporous silica	FA, BSA	PTX	ICG	635 nm, 100 mW cm <sup>-2</sup> , 10 min	Targets folate receptor-positive SGC-7901 cells, synergistic chemophotodynamic therapy (CI = 0.328), induces apoptosis	55
Xin Huang		GO, PEG	FA	DOX, TH287	ICG	808 nm, 1.0 W cm <sup>-2</sup> , 5 min	Kills MNNG/HOS/U2OS cells (IC <sub>50</sub> = 1.5 μg mL <sup>-1</sup> ), inhibits colony formation/migration, induces apoptosis/autophagy, reduces tumor weight/volume in nude mice	60



Table 3 (Contd.)

Researchers	Strategy	Nanomaterials	Tumor cell-targeting ligands	Loaded drugs	Photosensitizer	Laser parameters	Experimental results	Reference
Shouliang Lu		GO,PEG	FA	Rg3	ICG	808 nm, /, 2 min	Inhibits proliferation/ invasion of MG63/U2OS cells, reduces cancer stem cell stemness, inhibits tumor growth in nude mice (enhanced by NIR)	63
Haoyue Xu		P-(Nis)25	Angiopp -2	DOX	ICG	808 nm, 1.0 W cm <sup>-2</sup> , 5 min	Fluorescence-guided glioma surgery, postoperative PDT/PTT/ chemotherapy inhibits recurrence, median survival 72 days, no organ damage	65
Xueqing Zhang		Mesoporous silica	ApSF	DOC	ICG	808 nm, 2.0 W cm <sup>-2</sup> , 3 min	Synergistic PTT/PDT/ chemotherapy on 4T1 cells (viability 30.2%), induces ICD, 87.5% tumor inhibition, reduces lung metastasis, activates systemic immunity	61
Xiaoyi Hu		—	—	Osi	ICG	808 nm, 2.0 W cm <sup>-2</sup> , 3 min	Targets EGFR-positive NSCLC cells, induces apoptosis/autophagy/ ferroptosis (2x cell death vs. ICG), >96h tumor retention, inhibits growth with no systemic toxicity	66
Peilian Liu		—	Quinone propionic acid	Ir	ICG	808 nm, 1.0 W cm <sup>-2</sup> , 5 min	NQO1-responsive killing of A549 cells (apoptosis 69.10%), photothermal effect (tumor temp >60 °C), inhibits growth/ metastasis, 100% 50 days survival	68
Haoyu Guo		PDA	cRGD	TPZ	ICG	808 nm, 2.0 W cm <sup>-2</sup> , 4 min	Kills MNNG/HOS/U2OS cells (IC50 = 0.7249 μg mL <sup>-1</sup> ), inhibits migration, improves tumor hypoxia, reduces tumor weight per volume, hemolysis <5%	70

uses PDT to disrupt the tumor's vascular structure and inhibit tumor growth. This dual mechanism effectively reduces tumor blood supply and further enhances ICG's antitumor efficacy through PDT.

Another strategy involves co-loading ICG with bioactive molecules into nanoparticles. By encapsulating L-arginine (L-Arg) along with ICG in PLGA nanoparticles, ROS generated by ICG under near-infrared light not only kills tumor cells but also oxidizes L-Arg to produce nitric oxide (NO).<sup>47</sup> NO further reacts with ROS to form highly toxic reactive nitrogen species,<sup>48</sup> which activate matrix metalloproteinases (MMPs), thereby degrading

collagen in the tumor stroma and enhancing nanoparticle permeability within the tumor.<sup>49</sup> Additionally, some studies have combined nanoparticles with cell-penetrating peptides (TAT) to further boost the antitumor effect.<sup>50</sup> TAT can carry ICG across the cell membrane and into the nucleus,<sup>51</sup> where, under near-infrared light, ROS generation and temperature elevation induce DNA damage, leading to irreversible apoptosis.

Nanotechnology can also be combined with immunotherapy to form "active" nanoparticle delivery systems. By loading ICG onto carbon nanoparticles and modifying them with macrophages, researchers have developed a delivery platform capable



of activating immune responses.<sup>52</sup> Activated macrophages release pro-inflammatory cytokines, further enhancing the antitumor immune response.<sup>53</sup> When combined with ROS-induced cell damage, this approach significantly improves therapeutic outcomes. These functional recombination strategies have greatly expanded the application of ICG in nanomedicine, addressing its inherent stability issues and significantly enhancing its antitumor targeting and efficacy.

### 3.2 Organic polymer nanoparticles loaded with chemotherapeutic drugs

Although surgery combined with radiotherapy and chemotherapy remains the primary approach for cancer treatment, the side effects and low targeting ability of chemotherapy cause significant damage to normal cells. The advent of nanoscale drug delivery systems offers new possibilities for chemotherapy. By loading chemotherapeutic drugs into nanoparticles and incorporating photosensitizers, integrated approaches combining photoacoustic imaging, precision chemotherapy, and PDT can be achieved. This not only reduces side effects but also significantly enhances antitumor efficacy, advancing the development of combined cancer therapies.<sup>54</sup>

For example, hollow mesoporous silica nanoparticles (HMSNs) coated with folic acid-modified bovine serum albumin (FA-BSA) have been used to load ICG and paclitaxel (PTX).<sup>55</sup> The high expression of folic acid receptors in tumor cells allows this system to improve drug delivery precision through folic acid targeting.<sup>56</sup> Paclitaxel, a commonly used chemotherapeutic drug, faces reduced absorption in tumor cells due to *P*-glycoprotein (*P*-gp)-mediated efflux.<sup>57</sup> These nanoparticles enhance drug concentration at the tumor site *via* the EPR effect, thereby improving antitumor efficacy.<sup>58</sup>

Doxorubicin (DOX) is a widely used chemotherapeutic drug that induces DNA damage by intercalating into DNA and disrupting topoisomerase-mediated DNA repair, while also increasing intracellular ROS levels.<sup>59</sup> A type of functionalized graphene oxide (GO) nanoparticle has been developed to co-load the MTH1 inhibitor (TH287) and DOX,<sup>60</sup> which demonstrates strong synergy with ICG. Under near-infrared light, this system generates a photothermal effect that significantly enhances ROS production, increasing tumor cell sensitivity to ROS and improving the efficacy of PDT. Additionally, researchers have modified nanoparticles with *Antheraea pernyi* silk fibroin (ApSF).<sup>61</sup> During the functionalization with ApSF, ICG derivatives selectively target and disrupt tumor cell mitochondria, inducing apoptosis.<sup>62</sup> Similar studies have shown that ginsenoside Rg3 can also inhibit the migration of cancer stem cells *via* nanoparticle carriers, further enhancing the antitumor effect.<sup>63</sup> Furthermore, poly(nitroimidazole)<sub>25</sub> (*P*-(Nis)<sub>25</sub>) nanoparticles have been utilized as hypoxia-responsive carriers, capable of depolymerizing under hypoxic conditions to improve drug release efficiency.<sup>64</sup> These nanoparticles, loaded with both ICG and DOX, are further modified with the glioma-targeting peptide Angiopp-2, enabling them to cross the blood-brain barrier and precisely target gliomas, thereby achieving highly effective treatment of brain tumors.<sup>65</sup>

Another study demonstrated that nanoparticles formed by  $\pi$ - $\pi$  stacking of ICG and osimertinib (Osi) significantly improved the treatment efficacy of non-small cell lung cancer (NSCLC).<sup>66</sup> Osimertinib, a selective epidermal growth factor receptor (EGFR) inhibitor, combined with ICG, exhibited a strong photothermal effect in PDT. This combination enhanced antitumor activity by downregulating GPX4 and P62 and upregulating Caspase-3 and Beclin1 expression.<sup>67</sup> Similarly, another study developed a nanoparticle prodrug system based on the chemotherapeutic drug irinotecan (Ir) for NSCLC treatment.<sup>68</sup> This prodrug utilized quinone propionic acid, which is highly sensitive to the overexpressed quinone oxidoreductase-1 (NQO1) in NSCLC cells, thereby improving tumor cell targeting and antitumor efficacy.<sup>69</sup>

Lastly, a nanoparticle system using mesoporous polydopamine (PDA) as a carrier to load ICG and tirapazamine (TPZ) was developed.<sup>70</sup> This system achieved dual effects of homotypic targeting and active targeting through tumor cell membrane camouflage and cyclic Arg-Gly-Asp (cRGD) peptide modification.<sup>71</sup> Under laser irradiation, ICG activated and released ROS, exacerbating the hypoxic state of the tumor microenvironment. This hypoxia, in turn, activated the chemotherapeutic agent TPZ, generating transient oxidative radicals with selective toxicity against tumor cells.<sup>72</sup>

By loading chemotherapeutic drugs into organic polymer nanoparticles and combining them with photosensitizers and targeting molecules, the precision and antitumor efficacy of chemotherapy were significantly enhanced, while side effects on normal cells were substantially reduced. This provides a new solution for combined cancer therapy.

### 3.3 Organically modified metal (oxide) nanozymes

Nanozymes are artificial enzymes that possess the unique properties of nanomaterials along with catalytic functions, distinguishing them from natural and chemical enzymes. Composed of nanoparticles such as metals, metal oxides, and carbon-based materials, nanozymes are widely applied due to their high catalytic activity, stability, and cost-effectiveness.<sup>73</sup> The emergence of nanozymes has overturned the traditional view that inorganic nanomaterials are biologically inert, significantly expanding their range of applications. Currently, various types of nanozymes have been developed, including oxide nanozymes, noble metal nanozymes, carbon-based nanozymes, and metal-organic framework (MOF) nanozymes<sup>74,75</sup> (Table 4). These nanozymes catalyze the conversion of hydrogen peroxide (H<sub>2</sub>O<sub>2</sub>) into hydroxyl radicals ( $\cdot$ OH) or oxygen (O<sub>2</sub>), alleviating tumor hypoxia, enhancing antitumor efficacy, and exhibiting strong synergy with chemodynamic therapy (CDT).<sup>76</sup>

The unique characteristics of the tumor microenvironment, such as acidity, hypoxia, and high expression of H<sub>2</sub>O<sub>2</sub> and glutathione (GSH), significantly limit the effectiveness of traditional therapies. The core principle of CDT is the application of Fenton and Fenton-like reactions in the tumor microenvironment to convert excess H<sub>2</sub>O<sub>2</sub> into highly toxic  $\cdot$ OH, thereby enhancing the killing of tumor cells<sup>77</sup> (Fig. 4).





Table 4 Organic modified metal (oxide) nanodrugs

Researchers	Strategy	Nanomaterials	Tumor cell-targeting ligands	Fenton agent	Photosensitizer	Laser parameters	Experimental results	Reference
Xufeng Zhu	Enhance targeting capability	Mesoporous Silica, PEG	—	MnO <sub>2</sub>	ICG	808 nm, 2.0 W cm <sup>-2</sup> , 3 min	Targets HNE-1 nasopharyngeal carcinoma, GSH-responsive aggregation, synergistic PTT/PDT (86.5% cell death), inhibits <i>in vivo</i> tumor growth, good biocompatibility	78
Clare W. Teng	—	—	—	SPION	ICG, Ce6	665 nm, 5 mW cm <sup>-2</sup> , 16.4 min	For GL261 glioblastoma, fluorescence-guided PDT (10.1% <i>in vitro</i> viability), crosses blood-brain barrier, inhibits residual tumor growth	85
Ying Zhong	—	—	FA, CBT	SPION	ICG	808 nm, 0.98 W cm <sup>-2</sup> , 1 min	Targets HNE-1 nasopharyngeal carcinoma, GSH-responsive aggregation, synergistic PTT/PDT (86.5% cell death), nearly eradicates <i>in vivo</i> tumors, good biocompatibility	86
Xing Qin	—	—	LOx, CAT	Fe <sub>3</sub> O <sub>4</sub>	ICG	808 nm, 0.25 W cm <sup>-2</sup> , 5 min	Targets SMMC-7721 hepatoma cells, synergistic CDT/PDT (90% apoptosis), 89.05% <i>in vivo</i> tumor inhibition, no normal cell damage	83
Zixing Liang	—	MOF	—	Fe	ICG	808 nm, 1 W cm <sup>-2</sup> , 5 min	Targets EMT-6 cells, Fe-MOF-5+ICG, synergistic PDT/PTT (68.4% apoptosis), <i>in vivo</i> tumor inhibition, no organ toxicity at effective doses	90
Qing You	Improve ROS generation efficiency	MOF, Au	HSA	Pt	ICG	808 nm, 1.5 W cm <sup>-2</sup> , 5 min	Pt-based oxygen nanogenerator, multimodal imaging-guided PDT/PTT, 83% 45 days survival, inhibits metastasis, excellent biocompatibility	91
Shuo Qi	—	PDA, SH-PEG	CXCR 4 antibody	Pt	ICG	808 nm, 0.8 W cm <sup>-2</sup> , 10 min	CXCR4-targeted, HepG2/LM3 hepatoma cell killing, PTT/PDT (58.7% photothermal conversion), ablates small orthotopic tumors, no liver/kidney damage	92
Long Wen	—	—	BSA	MnO <sub>2</sub>	ICG	808 nm, 1 W cm <sup>-2</sup> , 5 min	Kills B16F10 melanoma cells, combined PTT-PDT (24.7% photothermal conversion), <i>in vivo</i> tumor regression, 100% survival rate, low toxicity	82
Xingyi Xu	—	—	Tumor cell membrane	Bi <sub>2</sub> O <sub>3</sub> , MnO <sub>2</sub>	ICG	808 nm, 0.8 W cm <sup>-2</sup> , 5 min	Targets TNBC, ICG loading 50.6%, mutually enhanced PTT/PDT/CDT (88% 4T1 cell death), significant <i>in vivo</i> tumor inhibition, excellent biocompatibility	81

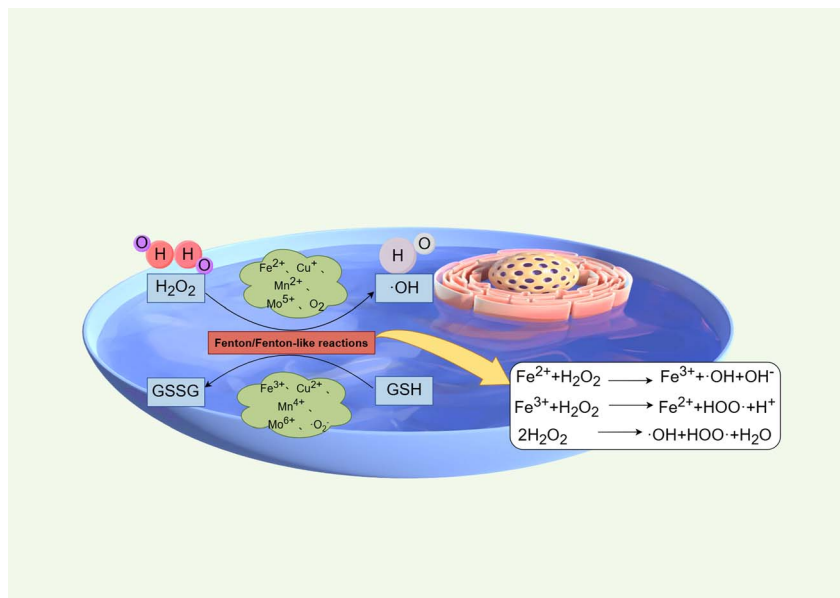


Fig. 4 The main mechanism of CDT. Essentially, CDT relies on the reaction between  $\text{Fe}^{2+}$  and  $\text{H}_2\text{O}_2$ . Specifically,  $\text{Fe}^{2+}$  reacts with  $\text{H}_2\text{O}_2$  to produce  $\cdot\text{OH}$ , and then the generated  $\text{Fe}^{3+}$  is reduced to  $\text{Fe}^{2+}$  by GSH, which is highly expressed in the TME.

Oxide nanozymes are the most widely used type of nanozyme. Manganese dioxide ( $\text{MnO}_2$ ) nanozymes can react with glutathione (GSH) to produce  $\text{Mn}^{2+}$ , which further catalyzes the conversion of  $\text{H}_2\text{O}_2$  into hydroxyl radicals ( $\cdot\text{OH}$ ).<sup>78</sup> *In vivo*,  $\text{MnO}_2$  decomposes into non-toxic  $\text{Mn}^{2+}$ , which is excreted through the kidneys, resulting in minimal side effects.<sup>79</sup> Additionally, the oxygen generated by  $\text{MnO}_2$  catalysis enhances ICG-mediated PDT by depleting GSH and reducing its scavenging of  $\cdot\text{OH}$  and singlet oxygen ( $^1\text{O}_2$ ), further improving therapeutic outcomes.<sup>80</sup> Researchers have also modified nanoparticles with biological components, such as tumor cell membranes<sup>81</sup> and bovine serum albumin,<sup>82</sup> to increase targeting specificity and retention time, yielding promising results. Iron oxide nanozymes exhibit pH-dependent properties, with a pronounced ability to catalyze the production of hydroxyl radicals from  $\text{H}_2\text{O}_2$  in the acidic tumor microenvironment. By integrating acidophilic lactate oxidase (LOX), catalase (CAT), which converts excess  $\text{H}_2\text{O}_2$  into water and oxygen, and ICG into  $\text{Fe}_3\text{O}_4$  nanoparticles, researchers have demonstrated strong antitumor potential under near-infrared light conditions.<sup>83</sup> Furthermore, magnetic iron oxide nanoparticles possess additional functions such as magnetic separation, magnetic resonance imaging, and magnetic hyperthermia. These nanoparticles have been validated as safe clinical agents and are widely applied in biomedicine.<sup>84</sup> For example, ICG and the second-generation photosensitizer Chlorin-e6 (Ce6) were attached to superparamagnetic iron oxide nanoparticles (SPIONs) and showed significant efficacy in combination with tumor-guided surgery for glioblastoma (GBM) treatment.<sup>85</sup> Additionally, 2-cyano-benzothiazole (CBT)-functionalized peptide-labeled aldehyde sodium alginate-coated magnetic iron oxide nanoparticles reacted with GSH to form intracellular aggregates, increasing the local concentration of the nanodrug.<sup>86</sup>

MOF nanozymes are a class of porous nanoparticles formed by bridging metal ions with organic ligands.<sup>87,88</sup> These nanozymes not only possess a porous structure but also exhibit enzyme-like activity, enabling them to integrate drug delivery, CDT, and other therapeutic modalities.<sup>89</sup> For example, Fe-MOF-5 nanoparticles have been used to load ICG, with the Fe element in the MOF catalyzing the conversion of hydrogen peroxide into oxygen, improving the hypoxic tumor microenvironment and enhancing the efficacy of PDT.<sup>90</sup> Other studies have modified MOF structures with platinum (Pt) nanozymes, which continuously decompose endogenous  $\text{H}_2\text{O}_2$  to generate  $\text{O}_2$ , creating an oxygen-enriched nanopatform that further boosts antitumor effects.<sup>91</sup>

Similarly, research has shown that encapsulating Pt in melanin-derived polydopamine (PDA) nanoparticles, combined with ICG and modified with a CXCR4 antibody targeting hepatocellular carcinoma (HCC), forms HCC-targeting nanoparticles.<sup>92</sup> These nanoparticles not only leverage the advantages of PDT but also enhance treatment efficacy through the catalytic activity of Pt, offering a new therapeutic strategy for difficult-to-treat cancers such as HCC. By integrating multiple functions, nanozymes demonstrate significant potential in cancer therapy, particularly when combined with PDT and CDT, as they can markedly improve therapeutic outcomes while minimizing damage to normal tissues.

### 3.4 Comprehensive nanoengineering strategies for overcoming the limitations of ICG in PDT

The integration of ICG into various nanocarriers is strategically designed to overcome its fundamental limitations, thereby unlocking its full potential for PDT. First, the nano-confinement effect within carriers like liposomes or polymeric nanoparticles physically separates ICG molecules, effectively preventing



concentration-dependent aggregation and the resultant quenching. This directly addresses the core issue of poor singlet oxygen yield by maintaining ICG in its photoactive monomeric state. Concurrently, the nano-encapsulation itself provides a protective barrier, significantly enhancing ICG's photostability and circulatory half-life. Furthermore, nanocarriers endow passive and active targeting capabilities. Their optimal size exploits the EPR effect for initial tumor accumulation, while surface functionalization with targeting ligands enables specific cellular uptake, which collectively enhance treatment specificity and reduce off-target effects. Finally, the most advanced nano-platforms transcend simple delivery by co-loading ICG with other therapeutic agents (*e.g.*, chemotherapeutics) or by leveraging its inherent mild photothermal effect. This facilitates combinatorial regimens, such as PDT/PTT/chemotherapy, where the photothermal effect can improve tumor oxygenation and drug permeability, creating a powerful synergistic anti-tumor outcome that single-modal therapies cannot achieve.

What makes ICG-based PDT combined with nanotechnology particularly compelling is its potential for image-guided immunomodulatory PDT: NIR fluorescence and photoacoustic properties of ICG enable real-time visualization of nanocarrier accumulation, drug release kinetics, and the release of DAMPs linked to ICD, thereby allowing dynamic adjustment of light dosage and treatment duration for each individual patient. In essence, advanced ICG-loaded nanocarriers are not merely delivery vehicles, but integrated theranostic systems that integrate targeted drug release, precision PDT, and immune activation, paving the way for next-generation cancer therapies that are more effective, safer, and tailored to the unique biological characteristics of each tumor.

#### 4. ICG-based PDT combined with nanotechnology and synergistic immunotherapy

During the PDT process, the photosensitizer itself exerts a weak cytotoxic effect on tumor cells, causing the lysis and death of a small portion of tumor cells, which releases tumor-associated antigens (TAAs) and triggers an immune response. However, this effect is minimal because TAAs alone, without additional adjuvants to recruit and activate antigen-presenting cells, generally fail to elicit an effective tumor immune response.<sup>15</sup> The greatest value of PDT lies not in its direct cytotoxicity, but in its ability to remodel the tumor microenvironment, converting immune "cold" tumors into "hot" tumors, thereby facilitating other treatment modalities.<sup>93</sup> In recent years, an increasing number of studies have found that combining PDT with immunotherapy produces significant synergistic effects. This combined treatment strategy not only enhances antitumor efficacy but also overcomes the limitations of monotherapies.

The first scientific attempts to use immunotherapy for cancer treatment are credited to two German physicians, Fehleisen and Busch, who observed tumor regression following erysipelas infections and conducted studies based on this

phenomenon. Later, William Bradley Coley, known as the father of immunotherapy, first used immunotherapy to treat bone sarcoma in 1891.<sup>94</sup> Today, with advanced technology, immunotherapy has become a cornerstone of clinical practice. The clinical goal of cancer immunotherapy is to activate the host's immune system, increase immune infiltration in the tumor microenvironment, and enhance the innate or specific immune response against malignancies.<sup>95</sup> Several immunotherapies, such as immune checkpoint inhibitors (ICIs), cancer vaccines, adoptive cell transfer (ACT), and oncolytic virus therapy (OVT), have already been applied in clinical practice and have shown promising results.<sup>96</sup>

PDT can effectively reduce tumor volume and promote antigen release through its direct tumor-killing action. Meanwhile, immunotherapy activates a systemic immune response, providing long-term control of tumor recurrence and metastasis. PDT enhances the ability of the immune system to recognize and attack tumors by providing more targeted antigens for immunotherapy.<sup>30</sup> The activation of T cells is crucial for a durable antitumor immune response and is the foundation for the success of combined PDT and immunotherapy. PDT induces ICD, and the tumor antigens and DAMPs produced by the dying tumor cells promote the recruitment and maturation of antigen-presenting cells (APCs). These APCs deliver tumor antigens to lymph nodes and activate CD8+ T cells, inducing an antitumor immune response that inhibits tumor growth and reduces the risk of metastasis.<sup>97</sup> Therefore, PDT can induce ICD, and ICD, in turn, enhances the efficacy of PDT. Additionally, studies have shown that nanotechnology can deliver exogenous immune adjuvants together with the photosensitizer ICG to the tumor microenvironment. For instance, aluminum hydroxide can capture antigens through electrostatic adsorption, ligand exchange, or water transport mechanisms, forming an antigen reservoir that enhances antigen presentation and immune response efficiency.<sup>98</sup>

Immune checkpoint inhibitors (such as PD-1/PD-L1 and CTLA-4 inhibitors) are one of the key modalities in immunotherapy, working by blocking tumor-induced T cell suppression and restoring T cell antitumor activity.<sup>99</sup> However, in "cold" tumors, where immune cell infiltration is insufficient, the response to immune checkpoint inhibitors is often poor. PDT, through its induced local inflammatory response and antigen release, attracts immune cell infiltration into the tumor region, converting immune "cold" tumors into "hot" tumors and thereby significantly enhancing the efficacy of immune checkpoint inhibitors. Currently, the combination of PDT and immunotherapy is rapidly advancing in both preclinical and clinical research. Many animal model studies have demonstrated that combining PDT with PD-1/PD-L1 inhibitors or CTLA-4 inhibitors can significantly improve antitumor efficacy.<sup>100</sup> For example, in murine tumor models, the group treated with PDT combined with PD-1 inhibitors showed stronger tumor suppression and prolonged survival.<sup>101</sup> Additionally, several clinical trials are underway to explore the combined use of PDT and immune checkpoint inhibitors, particularly in patients with advanced and metastatic cancers. Clinical trials focusing on head and neck tumors and non-small cell lung



cancer are assessing the synergistic effects of PDT and PD-1/PD-L1 inhibitors.<sup>101</sup>

Although immune checkpoint inhibitors have shown significant efficacy in certain tumor types, many patients experience resistance or lack of response to these therapies.<sup>102</sup> PDT, by activating innate and adaptive immune responses, can improve the responsiveness of these resistant tumors to immunotherapy, thereby expanding the population eligible for immunotherapy.<sup>103</sup> In the future, the combination of PDT and immunotherapy may evolve into personalized treatment regimens. Different strategies could be tailored based on the characteristics of the tumor's immune microenvironment (e.g., "cold" or "hot" tumors).<sup>35</sup> For instance, patients with "cold" tumors might first undergo PDT to modify the tumor microenvironment, followed by immune checkpoint inhibitors to achieve greater therapeutic efficacy. With the development of novel photosensitizers and nanotechnology, the effectiveness of PDT is expected to improve further. New photosensitizers are likely to target tumor cells more efficiently, reduce side effects, and exhibit even greater synergy with immunotherapy.<sup>30</sup> Future research may focus on developing more effective combinations of photosensitizers and immune modulators to enhance the efficacy of combination treatments. The synergy between PDT and immunotherapy holds promise as a more potent approach to cancer treatment.

## 5. Summary and outlook

PDT, when combined with nanotechnology, chemotherapy, and immunotherapy, holds the potential to evolve into a transformative cancer treatment strategy. Traditional PDT exerts its therapeutic effects by generating ROS to induce tumor cell death and remodel the immunosuppressive tumor microenvironment; notably, its combination with nanotechnology has garnered particular attention for its ability to convert "cold" tumors into "hot" ones. This synergistic effect activates both innate and adaptive immune responses, enhances antitumor efficacy, and extends its applicability to tumor types that were originally non-responsive. For ICG-based formulations, their inherent advantages render them an ideal platform for combinatorial immunotherapeutic PDT. These advantages include approval by FDA for clinical diagnostic applications, which lays a solid regulatory foundation for its repurposing as a therapeutic photosensitizer. Its NIR excitation property minimizes phototoxicity to normal tissues and enables the integration of imaging and therapeutic functions, thereby achieving real-time treatment monitoring. Nanocarrier-encapsulated ICG further improves tumor accumulation *via* the EPR effect; upon NIR light irradiation, it acts as a potent inducer of ICD, releasing DAMPs to activate dendritic cells (DCs) and initiate systemic antitumor immune responses. Nanocarrier encapsulation further enhances the stability, tumor-targeting efficiency, and ICD-inducing capacity of ICG, while the excellent synergistic compatibility of ICG-based PDT with chemotherapy and immunotherapy broadens its therapeutic application scenarios. Collectively, these advances have positioned ICG-based nano-platforms as promising candidates for bridging preclinical

innovation and clinical translation of combinatorial PDT-chemotherapy-immunotherapy.

However, the clinical translation of nanomedicine-aided ICG photodynamic therapy (ICG-PDT) and its combination with chemotherapy and immunotherapy still faces multiple interconnected challenges. Technically, the inherent photobleaching property of ICG limits the sustained generation of ROS during PDT; the penetration depth of NIR light remains insufficient to cover large or deep-seated tumors. From a regulatory and manufacturing perspective, scaling up the production of nanocarriers in compliance with Good Manufacturing Practice (GMP) standards remains a major hurdle, as it requires strict control over batch-to-batch consistency of physicochemical properties (e.g., particle size, zeta potential, drug loading efficiency) and long-term stability under storage conditions. Furthermore, regulatory authorities mandate comprehensive safety and efficacy data packages for novel combination products, a process that is both time-consuming and resource-intensive. Beyond these translational barriers, gaps persist in basic research, including incomplete elucidation of nanoparticle biosafety profiles, potential long-term immunogenicity risks, and the lack of standardized protocols for evaluating ICG-PDT efficacy in preclinical models. Despite encouraging preclinical findings, most ICG-based PDT systems still lack robust clinical data to support their widespread validation and application.

A critical aspect of accelerating the translational application of ICG-based PDT lies in addressing regulatory and GMP challenges by drawing on established precedents. Currently, several PDT products have obtained approval from FDA, providing valuable frameworks for the development of ICG-based systems. For instance, Photofrin, approved for the treatment of esophageal and lung cancers, had its core approval basis consisting of comprehensive *in vitro* data, *in vivo* studies, and rigorous phototoxicity assessments. For ICG-based PDT systems, existing preclinical studies have reported comparable *in vitro* ROS generation and ICD-inducing efficiency, as well as favorable *in vivo* tumor suppression efficacy in murine models. Nevertheless, critical gaps remain in standardized phototoxicity testing, long-term biosafety data, and standardized protocols for evaluating ICG-PDT efficacy in preclinical models—such as nanoparticle clearance pathways and immunogenicity profiles—which are essential to meet FDA requirements. To fill this gap, future efforts should focus on optimizing scalable GMP-compliant manufacturing processes (e.g., continuous flow synthesis and microfluidic technology) and conducting regulatory-compliant preclinical studies to generate comprehensive data packages that support Investigational New Drug (IND) applications.

To systematically overcome the aforementioned challenges, we propose targeted suggestions addressing key bottlenecks. First, to tackle the limitation of insufficient light penetration depth, develop NIR-II excited ICG nanocomposites or combine PDT with focused ultrasound technology to enhance light delivery in deep tissues. Second, to surmount the barriers to GMP-scale production, adopt modular manufacturing platforms and real-time quality control technologies (e.g., inline



particle sizing) to ensure batch consistency. Third, to address tumor heterogeneity, integrate predictive biomarkers including hypoxia-inducible factor 1 $\alpha$  and PD-L1 expression, and implement image-guided drug delivery to achieve personalized treatment. Fourth, to facilitate regulatory compliance, leverage FDA breakthrough therapy designation or orphan drug designation to expedite the approval process for ICG-based PDT systems.

From a commercialization perspective, the practical clinical implementation of ICG-based PDT hinges on balancing technological innovation and market feasibility. A viable translational pathway is to initially target localized, superficial tumors such as skin cancer and oral squamous cell carcinoma, where light delivery is less challenging and clinical endpoints can be rapidly evaluated. This strategy reduces the complexity and cost of initial clinical trials, facilitating early proof-of-concept validation. For deep-seated tumors, establishing partnerships with medical device companies to co-develop customized NIR light delivery systems (e.g., endoscopic light applicators) can enhance product competitiveness and clinical applicability. In addition, positioning ICG-based PDT as an adjuvant therapy to chemotherapy or immunotherapy can expand its market access, as it partially addresses the clinical challenge of “cold tumors”. Cost control is another critical factor for commercial success; scaling up nanocarrier production *via* GMP-compliant processes and exploring generic formulations after patent expiration can help improve affordability and market penetration.

In conclusion, empowered by nanotechnology and immunotherapy, ICG-based PDT holds tremendous potential to revolutionize cancer treatment. Despite significant challenges in translation, manufacturing, and regulation, a strategic approach integrating SWOT-guided research and development, regulatory precedent-based data generation, and market-oriented product design will pave the way for its clinical application. Future research should prioritize the development of standardized preclinical models, GMP-compliant manufacturing technologies, and patient-centric treatment strategies to fully unlock the translational potential of this highly promising therapeutic modality.

## Author contributions

All authors made a significant contribution to the work reported, whether that is in the conception, study design, execution, acquisition of data, analysis and interpretation, or in all these areas; took part in drafting, revising or critically reviewing the article; gave final approval of the version to be published; have agreed on the journal to which the article has been submitted; and agree to be accountable for all aspects of the work. All authors have read and agreed to the published version of the manuscript. All authors have read and agreed to the published version of the manuscript.

## Conflicts of interest

The authors declare that they have no competing interests.

## Data availability

No data were generated or analyzed in this study. Therefore, data sharing is not applicable to this article.

## Acknowledgements

The Figures were created by figdraw.

## References

- 1 F. Bray, M. Laversanne, H. Sung, J. Ferlay, R. L. Siegel, I. Soerjomataram and A. Jemal, *CA Cancer J. Clin.*, 2024, **74**, 229–263.
- 2 B. Liu, H. Zhou, L. Tan, K. T. H. Siu and X.-Y. Guan, *Signal Transduct. Targeted Ther.*, 2024, **9**, 175.
- 3 K. S. Rallis, T. H. Lai Yau and M. Sideris, *Anticancer Res.*, 2021, **41**, 1–7.
- 4 X. Li, J. F. Lovell, J. Yoon and X. Chen, *Nat. Rev. Clin. Oncol.*, 2020, **17**, 657–674.
- 5 H. Abrahamse and M. R. Hamblin, *Biochem. J.*, 2016, **473**, 347–364.
- 6 M. Olszowy, M. Nowak-Perlak and M. Woźniak, *Pharmaceutics*, 2023, **15**, 1712.
- 7 C. Kong and X. Chen, *Int. J. Nanomed.*, 2022, **17**, 6427–6446.
- 8 F. Esperou, M. Lorusso, A. Santarelli, A. De Lillo, L. Lo Muzio, D. Ciavarella and L. Lo Russo, *Front. Oncol.*, 2025, **15**, 1619560.
- 9 S. Lam, *Semin. Oncol.*, 1994, **21**, 15–19.
- 10 J. Lin, L.-S. Lin, D.-R. Chen, K.-J. Lin, Y.-F. Wang and Y.-J. Chang, *Asian J. Surg.*, 2020, **43**, 1149–1153.
- 11 D. M. Dereje, C. Pontremoli, M. J. Moran Plata, S. Visentin and N. Barbero, *Photochem. Photobiol. Sci.*, 2022, **21**, 397–419.
- 12 S. Singh, G. Giammanco, C.-H. Hu, J. Bush, L. S. Cordova, D. J. Lawrence, J. L. Moran, P. V. Chitnis and R. Veneziano, *Photoacoustics*, 2023, **29**, 100437.
- 13 N. Kwon, H. Weng, M. A. Rajora and G. Zheng, *Angew Chem. Int. Ed. Engl.*, 2025, **64**, e202423348.
- 14 A. S. Thakor and S. S. Gambhir, *CA Cancer J. Clin.*, 2013, **63**, 395–418.
- 15 B. Ji, M. Wei and B. Yang, *Theranostics*, 2022, **12**, 434–458.
- 16 *Nanoparticles in Biology and Medicine: Methods and Protocols*, ed. E. Ferrari and M. Soloviev, Springer US, New York, NY, 2020, vol. 2118.
- 17 D. Dinakaran and B. C. Wilson, *Front. Bioeng. Biotechnol.*, 2023, **11**, 1250804.
- 18 H. Maeda, J. Wu, T. Sawa, Y. Matsumura and K. Hori, *J. Control. Release*, 2000, **65**, 271–284.
- 19 Y. Hou, X. Yang, R. Liu, D. Zhao, C. Guo, A. Zhu, M. Wen, Z. Liu, G. Qu and H. Meng, *Int. J. Nanomed.*, 2020, **15**, 6827–6838.
- 20 N. Sobhani, A. A. Samadani and J. Egypt, *J. Natl. Cancer Inst.*, 2021, **33**, 34.
- 21 K. Plaetzer, B. Krammer, J. Berlanda, F. Berr and T. Kiesslich, *Laser Med. Sci.*, 2009, **24**, 259–268.



- 22 M. S. Baptista, J. Cadet, P. Di Mascio, A. A. Ghogare, A. Greer, M. R. Hamblin, C. Lorente, S. C. Nunez, M. S. Ribeiro, A. H. Thomas, M. Vignoni and T. M. Yoshimura, *Photochem. Photobiol.*, 2017, **93**, 912–919.
- 23 S. Sellevold, Q. Peng, A. S. V. Fremstedal and K. Berg, *Photodiagnosis Photodyn. Ther.*, 2017, **20**, 95–106.
- 24 W. Bu, S. Zhao, Q. Zhang, F. Fang and L. Yang, *Laser Med. Sci.*, 2022, **37**, 2865–2872.
- 25 R. R. Allison and S. Bansal, *Photodiagnosis Photodyn. Ther.*, 2022, **38**, 102825.
- 26 J. K. Kim, M. R. Byun, C. H. Maeng, Y. R. Kim and J. W. Choi, *Cancers*, 2020, **12**, 203.
- 27 L. Jiang, Y. Liu, X. Su, J. Wang, Y. Zhao, S. Tumbath, J. A. Kilgore, N. S. Williams, Y. Chen, X. Wang, M. S. Mendonca, T. Lu, Y.-X. Fu and X. Huang, *Front. Oncol.*, 2022, **12**, 976292.
- 28 J. Hua, P. Wu, L. Gan, Z. Zhang, J. He, L. Zhong, Y. Zhao and Y. Huang, *Front. Oncol.*, 2021, **11**, 738323.
- 29 L. Tan, X. Shen, Z. He and Y. Lu, *Front. Oncol.*, 2022, **12**, 863107.
- 30 Z. Liu, Z. Xie, W. Li, X. Wu, X. Jiang, G. Li, L. Cao, D. Zhang, Q. Wang, P. Xue and H. Zhang, *J. Nanobiotechnol.*, 2021, **19**, 160.
- 31 I. Beltrán Hernández, Y. Yu, F. Ossendorp, M. Korbelik and S. Oliveira, *J. Clin. Med.*, 2020, **9**, 333.
- 32 T. Dudzik, I. Domański and S. Makuch, *Front. Immunol.*, 2024, **15**, 1335920.
- 33 W. Chou, T. Sun, N. Peng, Z. Wang, D. Chen, H. Qiu and H. Zhao, *Pharmaceutics*, 2023, **15**, 2617.
- 34 V. D. Turubanova, I. V. Balalaeva, T. A. Mishchenko, E. Catanzaro, R. Alzeibak, N. N. Peskova, I. Efimova, C. Bachert, E. V. Mitroshina, O. Krysko, M. V. Vedunova and D. V. Krysko, *J. Immunother. Cancer*, 2019, **7**, 350.
- 35 J. Jia, X. Wu, G. Long, J. Yu, W. He, H. Zhang, D. Wang, Z. Ye and J. Tian, *Front. Immunol.*, 2023, **14**, 1219785.
- 36 N. Alvarez and A. Sevilla, *Int. J. Mol. Sci.*, 2024, **25**, 1023.
- 37 B. Ji, M. Wei and B. Yang, *Theranostics*, 2022, **12**, 434–458.
- 38 M. Geszke-Moritz and M. Moritz, *Polymers*, 2024, **16**, 2536.
- 39 Z. M. S. H. Khan, S. Saifi, Shumaila, Z. Aslam, S. A. Khan and M. Zulfeqar, *J. Photochem. Photobiol. Chem.*, 2020, **388**, 112201.
- 40 H. Mehravanfar, N. Farhadian and K. Abnous, *J. Drug Target.*, 2024, **32**, 820–837.
- 41 Y. Hu, R. Wang, Y. Zhou, N. Yu, Z. Chen, D. Gao, X. Shi and M. Shen, *J. Mater. Chem. B*, 2018, **6**, 6122–6132.
- 42 H. Ren, J. Liu, Y. Li, H. Wang, S. Ge, A. Yuan, Y. Hu and J. Wu, *Acta Biomater.*, 2017, **59**, 269–282.
- 43 L. Sitia, P. Saccomandi, L. Bianchi, M. Sevieri, C. Sottani, R. Allevi, E. Grignani, S. Mazzucchelli and F. Corsi, *Int. J. Nanomed.*, 2024, **19**, 4263–4278.
- 44 F. Chen, Y. Fan, J. Hou, B. Liu, B. Zhang, Y. Shang, Y. Chang, P. Cao and K. Tan, *Aging*, 2021, **13**, 21671–21699.
- 45 Y. Liu, S. Dai, L. Wen, Y. Zhu, Y. Tan, G. Qiu, T. Meng, F. Yu, H. Yuan and F. Hu, *Int. J. Nanomed.*, 2020, **15**, 2717–2732.
- 46 P. Zhang, L. Hu, Q. Yin, L. Feng and Y. Li, *Mol. Pharm.*, 2012, **9**, 1590–1598.
- 47 Z. Sun, X. Wang, J. Liu, Z. Wang, W. Wang, D. Kong and X. Leng, *Mol. Pharm.*, 2021, **18**, 928–939.
- 48 K. Zhang, H. Xu, X. Jia, Y. Chen, M. Ma, L. Sun and H. Chen, *ACS Nano*, 2016, **10**, 10816–10828.
- 49 X. Dong, H.-J. Liu, H.-Y. Feng, S.-C. Yang, X.-L. Liu, X. Lai, Q. Lu, J. F. Lovell, H.-Z. Chen and C. Fang, *Nano Lett.*, 2019, **19**, 997–1008.
- 50 J. Liu, Y. Yin, L. Yang, B. Lu, Z. Yang, W. Wang and R. Li, *Int. J. Nanomed.*, 2021, **16**, 1473–1485.
- 51 D. M. Copolovici, K. Langel, E. Eriste and Ü. Langel, *ACS Nano*, 2014, **8**, 1972–1994.
- 52 X. Wang, J. Lu, Y. Mao, Q. Zhao, C. Chen, J. Han, M. Han, H. Yuan and S. Wang, *J. Controlled Release*, 2022, **347**, 14–26.
- 53 D. G. DeNardo and B. Ruffell, *Nat. Rev. Immunol.*, 2019, **19**, 369–382.
- 54 J. Yan, X. Long, Y. Liang, F. Li, H. Yu, Y. Li, Z. Li, Y. Tian, B. He and Y. Sun, *Colloids Surf. B Biointerfaces*, 2022, **217**, 112701.
- 55 Y. Zhang and Y. Liang, *Heliyon*, 2024, **10**, e29274.
- 56 Y. Wang, J. Zhang, X. Lv, L. Wang, Z. Zhong, D.-P. Yang, W. Si, T. Zhang and X. Dong, *Biomaterials*, 2020, **252**, 120111.
- 57 M. Habibi Jouybari, S. Hosseini, K. Mahboobnia, L. A. Boloursaz, M. Moradi and M. Irani, *Colloids Surf. B Biointerfaces*, 2019, **179**, 495–504.
- 58 H. Meng, M. Xue, T. Xia, Z. Ji, D. Y. Tarn, J. I. Zink and A. E. Nel, *ACS Nano*, 2011, **5**, 4131–4144.
- 59 S. H. Shin, Y. J. Choi, H. Lee, H.-S. Kim and S. W. Seo, *Tumor Biol.*, 2016, **37**, 1591–1598.
- 60 X. Huang, J. Chen, W. Wu, W. Yang, B. Zhong, X. Qing and Z. Shao, *Acta Biomater.*, 2020, **109**, 229–243.
- 61 X. Zhang, Q. He, J. Sun, H. Gong, Y. Cao, L. Duan, S. Yi, B. Ying and B. Xiao, *Adv. Healthc. Mater.*, 2022, **11**, 2200255.
- 62 H.-L. Xu, D.-L. ZhuGe, P.-P. Chen, M.-Q. Tong, M.-T. Lin, X. Jiang, Y.-W. Zheng, B. Chen, X.-K. Li and Y.-Z. Zhao, *Drug Deliv.*, 2018, **25**, 364–375.
- 63 S.-L. Lu, Y.-H. Wang, G.-F. Liu, L. Wang, Y. Li, Z.-Y. Guo and C. Cheng, *Front. Mol. Biosci.*, 2021, **8**, 663089.
- 64 H. Liu, Y. Xie, Y. Zhang, Y. Cai, B. Li, H. Mao, Y. Liu, J. Lu, L. Zhang and R. Yu, *Biomaterials*, 2017, **121**, 130–143.
- 65 H. Xu, Y. Han, G. Zhao, L. Zhang, Z. Zhao, Z. Wang, L. Zhao, L. Hua, K. Naveena, J. Lu, R. Yu and H. Liu, *ACS Appl. Mater. Interfaces*, 2020, **12**, 52319–52328.
- 66 X. Hu, J. Li, Y. Chen, Q. Long, Y. Bai, R. Li, K. Wang, M. Jiang, C. Chen, J. Mao, Y. Zheng and Z. Gao, *ACS Biomater. Sci. Eng.*, 2022, **8**, 4535–4546.
- 67 S. Wang, S. Cang and D. Liu, *J. Hematol. Oncol.*, 2016, **9**, 34.
- 68 P. Liu, Y. Huang, C. Zhan, F. Zhang, C. Deng, Y. Jia, T. Wan, S. Wang and B. Li, *Mater. Today Bio*, 2023, **21**, 100722.
- 69 K. Wang, X. Xiao, Y. Liu, Q. Zong, Y. Tu and Y. Yuan, *Biomaterials*, 2022, **289**, 121803.
- 70 H. Guo, L. Wang, W. Wu, M. Guo, L. Yang, Z. Zhang, L. Cao, F. Pu, X. Huang and Z. Shao, *J. Controlled Release*, 2022, **351**, 151–163.
- 71 A. Sheikh, S. Md and P. Kesharwani, *J. Controlled Release*, 2021, **340**, 221–242.



- 72 D. Guo, S. Xu, W. Yasen, C. Zhang, J. Shen, Y. Huang, D. Chen and X. Zhu, *Biomater. Sci.*, 2020, **8**, 694–701.
- 73 N. Alizadeh and A. Salimi, *J. Nanobiotechnol.*, 2021, **19**, 26.
- 74 S. K. T, M. N. D. Bs, L. R. Babu, A. E. Paul, S. Murugan and R. Periakaruppan, *J. Clust. Sci.*, 2024, **35**, 715–740.
- 75 T. Luo, Y. Fan, J. Mao, E. Yuan, E. You, Z. Xu and W. Lin, *J. Am. Chem. Soc.*, 2022, **144**, 5241–5246.
- 76 S. Jeyachandran, R. Srinivasan, T. Ramesh, A. Parivallal, J. Lee and E. Sathiyamoorthi, *Biomimetics*, 2023, **8**, 446.
- 77 C. Cao, X. Wang, N. Yang, X. Song and X. Dong, *Chem. Sci.*, 2022, **13**, 863–889.
- 78 Y. Ju, B. Dong, J. Yu and Y. Hou, *Nano Today*, 2019, **26**, 108–122.
- 79 P. Wang, W. Yang, S. Shen, C. Wu, L. Wen, Q. Cheng, B. Zhang and X. Wang, *ACS Nano*, 2019, **13**, 11168–11180.
- 80 X. Zhu, Y. Liu, G. Yuan, X. Guo, J. Cen, Y. Gong, J. Liu and Y. Gang, *Nanoscale*, 2020, **12**, 22317–22329.
- 81 X. Xu, R. Zhang, X. Yang, Y. Lu, Z. Yang, M. Peng, Z. Ma, J. Jiao and L. Li, *Adv. Healthc. Mater.*, 2021, **10**, 2100518.
- 82 L. Wen, R. Hyoju, P. Wang, L. Shi, C. Li, M. Li and X. Wang, *Laser Surg. Med.*, 2021, **53**, 390–399.
- 83 X. Qin, C. Wu, D. Niu, L. Qin, X. Wang, Q. Wang and Y. Li, *Nat. Commun.*, 2021, **12**, 5243.
- 84 K. X. Vazquez-Prada, J. Lam, D. Kamato, Z. P. Xu, P. J. Little and H. T. Ta, *Arterioscler. Thromb. Vasc. Biol.*, 2021, **41**, 601–613.
- 85 C. W. Teng, A. Amirshaghghi, S. S. Cho, S. S. Cai, E. De Ravin, Y. Singh, J. Miller, S. Sheikh, E. Delikatny, Z. Cheng, T. M. Busch, J. F. Dorsey, S. Singhal, A. Tsourkas and J. Y. K. Lee, *J. Neuro-Oncol.*, 2020, **149**, 243–252.
- 86 Y. Zhong, N. K. Bejjanki, X. Miao, H. Weng, Q. Li, J. Zhang, T. Liu, R. Vannam and M. Xie, *Front. Bioeng. Biotechnol.*, 2021, **9**, 730925.
- 87 Z. Xu, T. Luo and W. Lin, *Acc. Mater. Res.*, 2021, **2**, 944–953.
- 88 I. Abánades Lázaro, X. Chen, M. Ding, A. Eskandari, D. Fairen-Jimenez, M. Giménez-Marqués, R. Gref, W. Lin, T. Luo and R. S. Forgan, *Nat. Rev. Methods Primers*, 2024, **4**, 42.
- 89 J. Liu, J. Huang, L. Zhang and J. Lei, *Chem. Soc. Rev.*, 2021, **50**, 1188–1218.
- 90 Z. Liang, X. Li, X. Chen, J. Zhou, Y. Li, J. Peng, Z. Lin, G. Liu, X. Zeng, C. Li, L. Hang and H. Li, *Front. Bioeng. Biotechnol.*, 2023, **11**, 1156079.
- 91 Q. You, K. Zhang, J. Liu, C. Liu, H. Wang, M. Wang, S. Ye, H. Gao, L. Lv, C. Wang, L. Zhu and Y. Yang, *Adv. Sci.*, 2020, **7**, 1903341.
- 92 S. Qi, G. Liu, J. Chen, P. Cao, X. Lei, C. Ding, G. Chen, Y. Zhang and L. Wang, *Int. J. Nanomed.*, 2022, **17**, 3777–3792.
- 93 J. Ni, Z. Zhang, M. Ge, J. Chen and W. Zhuo, *Acta Pharmacol. Sin.*, 2023, **44**, 288–307.
- 94 P. Dobosz and T. Dzieciatkowski, *Front. Immunol.*, 2019, **10**, 2965.
- 95 J. A. Marin-Acevedo, A. E. Soyano, B. Dholaria, K. L. Knutson and Y. Lou, *J. Hematol. Oncol.*, 2018, **11**, 8.
- 96 R. Rui, L. Zhou and S. He, *Front. Immunol.*, 2023, **14**, 1212476.
- 97 R. Alzeibak, T. A. Mishchenko, N. Y. Shilyagina, I. V. Balalaeva, M. V. Vedunova and D. V. Krysko, *J. Immunother. Cancer*, 2021, **9**, e001926.
- 98 X. Zhong, C. Li, G. Zhao, M. Li, S. Chen, Y. Cao, Q. Wang, J. Sun, S. Zhu and S. Chang, *J. Nanobiotechnol.*, 2022, **20**, 468.
- 99 M. Yang, M. Cui, Y. Sun, S. Liu and W. Jiang, *Cell Commun. Signal.*, 2024, **22**, 338.
- 100 A. Rotte, *J. Exp. Clin. Cancer Res.*, 2019, **38**, 255.
- 101 S. Qin, L. Xu, M. Yi, S. Yu, K. Wu and S. Luo, *Mol. Cancer*, 2019, **18**, 155.
- 102 M. Karasarides, A. P. Cogdill, P. B. Robbins, M. Bowden, E. M. Burton, L. H. Butterfield, A. Cesano, C. Hammer, C. L. Haymaker, C. E. Horak, H. M. McGee, A. Monette, N.-P. Rudqvist, C. N. Spencer, R. F. Sweis, B. G. Vincent, E. Wennerberg, J. Yuan, R. Zappasodi, V. M. H. Lucey, D. K. Wells and T. LaVallee, *Cancer Immunol. Res.*, 2022, **10**, 372–383.
- 103 X. Yang, W. Zhang, W. Jiang, A. Kumar, S. Zhou, Z. Cao, S. Zhan, W. Yang, R. Liu, Y. Teng and J. Xie, *J. Nanobiotechnol.*, 2021, **19**, 182.

